SEARCHES FOR COSMOLOGICAL GWs IN THE NANOGrav 15-YEAR DATASET*

Rafael R. Lino dos Santos

for the NANOGrav Collaboration
New Physics Working Group

National Centre for Nuclear Research (NCBJ), Warsaw, Poland

Received 31 March 2025, accepted 2 November 2025, published online 19 December 2025

In these proceedings, we report on the latest searches for cosmology and New Physics with the NANOGrav 15-year dataset. We focus on the model-independent running of the spectral index and comment on the cosmic-inflation interpretations reported in previous NANOGrav Collaboration papers.

DOI:10.5506/APhysPolBSupp.18.6-A8

1. Introduction

Over the past decade, we have seen the emergence of gravitational-wave (GW) and multi-messenger astronomy as successful probes of different regimes of gravity, starting with the seminal GW detections by the LIGO–Virgo collaboration in 2015 and 2017 [1, 2], from mergers of black-hole and neutron-star binaries, respectively. Also, we witnessed increasing efforts on detecting the (stochastic) gravitational wave background (GWB), through networks of pulsar timing arrays (PTAs) [3]: radio-telescopes on Earth observe and time the arrival of photons coming from millisecond pulsars in the galactic neighbourhood [4]. In turn, the target is the detection of a cross-correlation pattern — known as the Hellings–Downs (HD) correlation [5] — that a GWB induces in the correlated timing residuals of pairs of these millisecond pulsars. Along this line, in 2023, the main PTA collaborations released their latest datasets [6–9], in which, for the first time, we could see strong evidence for the HD correlation. In particular, the NANOGrav 15-year dataset (NG15) provided compelling evidence for a nanohertz (nHz) GWB with a statistical significance level of 3.5–4.0σ.

* Presented at the V4-HEP 4 — Theory and Experiment in High Energy Physics Workshop, Warsaw, Poland, 28–31 October, 2024.

While one knows what is the source of most of the GWs detected by LIGO–Virgo–KAGRA (LVK), the picture for PTAs is not entirely clear. On the one hand, we expect that the cosmic population of inspiralling supermassive black-hole binaries (SMBHB) is the main astrophysical source producing a GWB [10]. These supermassive objects are found in the centre of galaxies, and after the detection of shadows of compact objects by the EHT Collaboration [11] (the "black-hole images"), a next major step would be the detection of GWs from SMBHBs. On the other hand, if one tries to fit NG15 with simple SMBHB scenarios (for instance, if the GW spectrum is a power-law with spectral index $\gamma = 13/3$, see details below), one runs into problems explaining the data. That motivated an extensive search for self-consistent phenomenological binary and GW-driven models in [12], where we can see that it is possible to reconcile the HD signal present in NG15 with an astrophysical population of SMBHBs, see, for instance, Fig. 7 in [12].

A second perspective, not necessarily excluding the astrophysical source, is that the HD signal is also caused by a cosmological background, which was created by an extensive set of cosmological sources [13]. In this case, PTAs, together with LVK and future space-based missions like LISA, open a new discovery window for cosmology and New Physics beyond the Standard Model (BSM). Without GW experiments, one needs to rely on extrapolations from CMB scales towards the high-energy regimes relevant for model building in cosmology and BSM physics. That helps to understand why PTAs, LVK, and LISA are so well received by different physics communities. In this direction, in 2023, we performed an extensive search for signals of New Physics [14] with NG15. These included stochastic searches — namely, inflationary gravitational waves (IGW), scalar-induced gravitational waves (SIGW), first-order phase transitions, cosmic strings, and domain walls — and deterministic searches for ultralight dark matter and dark matter substructures. See [15] for the cosmological interpretation of EPTA DR2 data and [16, 17] for two other independent, extensive searches. Even though one does not yet have statistical significance to detect cosmological sources, new bounds and constraints were already established. Several works also prospect for a cosmological GWB in the LISA frequency range [18].

These proceedings are organised as follows. In Section 2, we discuss the GW characterisation of the GWB, paving the way for the description of the running power-law model explored in Section 3. Then, we make a few comments on the inflationary interpretations of NG15 in Section 4 and conclude in Section 5.

2. Gravitational wave characterisation

Here, we present some notions of GW characterisation. We mix notations from [19] and [20]. See more details, for *e.g.*, in [21]. Assuming the usual parametrisation for transverse and traceless tensor modes

$$h_{ij}(t,\vec{x}\,) = \sum_{a=+,\times} \int \frac{\mathrm{d}k}{(2\pi)} \int_{S^2} \mathrm{d}\Omega_{\hat{n}}\, H_a(k,\Omega)\, e^{i\,k_\mu x^\mu}\, \hat{e}^a_{ij}(\hat{n})\,, \tag{1}$$

with $k = 2\pi(f/a_0)$, and assuming a Gaussian, stationary, unpolarised, homogeneous, and isotropic background

$$\langle H_a(f_1,\Omega_1) H_b(f_2,\Omega_2)\rangle = \frac{1}{2}\delta_{ab}\frac{\delta(\Omega_1,\Omega_2)}{4\pi}(2\pi)\delta(f_1-f_2)S_h(f_1)\,, \tag{2}$$

where $S_h(f)$ is the one-sided power spectral density, we can write the cross-power spectral density of noise-free timing residuals (for a pair of pulsars i,j) as

$$S_{\mathrm{GW}}(f)_{ij} = \frac{S_h(f)}{12\pi^2 f^2}\Gamma_{\mathrm{HD},ij} = \frac{h_c^2(f)}{12\pi^2 f^3}\Gamma_{\mathrm{HD},ij}\,. \tag{3}$$

Here, $h_c(f) = \sqrt{f S_h(f)}$ is the characteristic GW strain amplitude, and the frequency-independent Hellings–Downs correlation is given by

$$\Gamma_{\mathrm{HD},ij} = \frac{1}{2}(1+\delta_{ij}) - \frac{1}{4}x_{ij} + \frac{3}{2}x_{ij}\ln x_{ij}\,, \tag{4}$$

for $x_{ij} = (1-\cos\xi_{ij})/2$ (pulsar angular separation). See, for instance [20], for a pedagogical derivation. In Eq. (3), we can see how the timing residuals depend on the source (through the strain $h_c(f)$) and on geometry (through the frequency-independent HD correlation). For a given source, using Eq. (2), we can calculate the GW energy density spectrum through

$$\Omega_{\mathrm{GW}} = \frac{1}{\rho_c}\frac{\mathrm{d}\rho_{\mathrm{GW}}(f)}{\mathrm{d}\ln f} = \frac{4\pi^2}{3H_0^2} f^3 S_h(f)\,. \tag{5}$$

Below, we report on two possible model-independent parameterisations.

2.1. Constant power law

The most standard prescription is to model the strain h_c with a single constant power-law (CPL) ansatz

$$h_c(x) = A\,x^\alpha \;\Rightarrow\; S^{\mathrm{CPL}}_{\mathrm{GW}}(x)_{ij} = \frac{A^2\Gamma_{\mathrm{HD},ij}}{12\pi^2 f_{\mathrm{ref}}^2} x^{-\gamma} \tag{6}$$

$$\Rightarrow\; \Omega^{\mathrm{CPL}}_{\mathrm{GW}}(x) = \frac{2\pi^2}{3H_0^2} A^2 f_{\mathrm{ref}}^2\, x^{5-\gamma}\,, \tag{7}$$

where $x \equiv \left(\frac{f}{f_{\rm ref}}\right)$ and $\gamma = 3-2\alpha$ is the spectral index. Here, we can identify the spectral index with the negative power of f in $S_{\rm GW}(f)_{ij}$, or with

$$\gamma_{\rm run}(x) = -\frac{{\rm d}\ln S_{\rm GW}(x)_{ij}}{{\rm d}\ln x}\,. \tag{8}$$

For CPL, that is just $\gamma_{\rm run}(x) \equiv \gamma$.

2.2. Running power law

If we want to allow the spectral index to run over frequencies, we need to be a bit careful on how to relate it with $\Omega_{\rm GW}(f)$. For instance, let us assume

$$\gamma_{\rm run}(x) = \gamma + \beta\,\ln x \tag{9}$$

as our starting point, then we can no longer write $S_{\rm GW}(f) \sim f^{-\gamma_{\rm run}}$. Indeed, we can show that $\ln(S_{\rm GW}^{\rm CPL} - S_{\rm GW}^{\rm RPL}) = (\beta/2)(\ln x)^2$ (notice the extra $1/2$ factor) [19]. For us, the GW energy density spectrum is

$$\Omega_{\rm GW}^{\rm RPL}(x) = \frac{2\pi^2}{3H_0^2} A^2 f_{\rm ref}^2\, x^{5-\left(\gamma+\frac{\beta}{2}\ln x\right)}\,. \tag{10}$$

If we consider the dependence of $\ln\Omega_{\rm GW}^{\rm RPL}$ over $\ln x$, we can see that the corresponding GW spectrum is parabolic, proportional to $(\ln x)^2$, while for $\ln\Omega_{\rm GW}^{\rm CPL}$, it is linear. Notice that the information of A and γ is only meaningful once one defines a reference frequency $f_{\rm ref}$. The physical information is contained in $\Omega_{\rm GW}$, which is invariant under change of $f_{\rm ref}$ (see the set of affine transformations relating the parameters (A, γ, β) at a given $f_{\rm ref}$ in [19]).

3. NG15: The running power-law model

If one starts from a particular model, one can derive the GW spectrum for that source (top-down), but one could also think of a bottom-up approach to characterise the signal, without prior information about the source. In [19], we developed a first model-independent spectral characterisation in the PTA band that departs from *(i)* the simplest CPL models, *e.g.*, simple power-law or broken power-law spectra; and *(ii)* the free spectrum approach, in which the GWB amplitude is treated as a free parameter for each frequency bin in the dataset. Phenomenologically, one would also expect that the RPL ansatz could also reproduce astrophysical scenarios predicting a spectral turnover at low frequencies or cosmological scenarios yielding a mild running

of the spectral index. In [19], we performed the first Bayesian analysis with the RPL parameters (A, γ, β) in Eq. (10) with NG15 data using PTArcade [22, 23] in enterprise mode [24, 25].

Our Bayesian analysis followed the same methods as in the previous search for New Physics [14]. We were able to derive Bayesian limits for the amplitude A, the spectral index γ, and the running of the spectral index β at $f = f_{\rm ref}$. Let us summarise here the main results that can also be observed in Fig. 1. In the corner plot on the left-hand side, we can see, in blue, the marginalised 2D and 1D posterior densities derived from the 3D posterior. From these posterior densities, we obtained the point of the highest 3D posterior density (maximum *a posteriori* (MAP) point), and the 68% and 95% credible intervals (credible regions) obtained from the 1D (2D) densities. From the 3D density, we obtain credible bands corresponding to the highest-posterior-density volumes using kernel density approximation. With green and cyan circle markers, we show the projection in 2D space of a sample of 100 triples of RPL parameters that are inside the 68% and 95% credible bands. Then, in the plot on the right-hand side, we can see different GWB spectra. The orange line corresponds to the one predicted by the MAP point. The green and cyan lines are the ones predicted by the same sample of 100 triples of RPL parameters that are inside the 68% (dark blue) and 95% (light blue) credible bands, respectively.

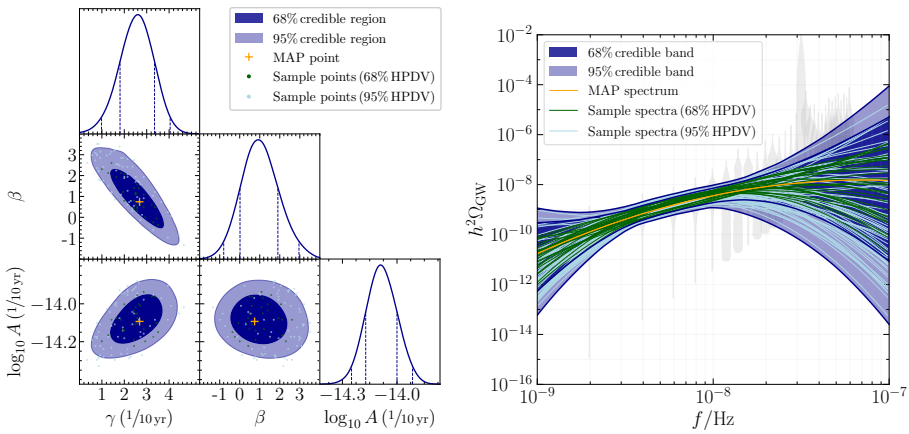

Fig. 1. Left panel: corner plot of the 3D parameter space of the RPL model. Right panel: GWB spectra predicted by samples of RPL parameters. From [19].

All the priors, points and interval estimates for the RPL model can be found in Tables 1 and 2 of [19]. Here, we quote one of the main results: the 1D MAP point for running of the spectral index is $\beta = 0.92^{+0.98\,(+2.04)}_{-0.91\,(-1.72)}$, with error bars corresponding to the 68% (95%) credible interval. This is

still consistent with no running, but we can see that the 68% interval itself does not include $\beta = 0$. Additionally, we also performed a model comparison between the RPL and CPL models. In this case, we found a Bayes factor (BF) of 0.69 ± 0.01 (RPL/CPL). This BF slightly favours the CPL model (which might be attributed to the smaller prior volume in CPL), but cannot be used to indicate preference for any of the models. The RPL model did not significantly improve the quality of the fit of NG15. Future datasets may lead to a non-zero measurement of β.

4. NG15: Inflationary gravitational waves

As a proof-of-concept, we show how we can use PTA data to probe cosmology with inflationary gravitational waves (IGW). If one wants to fit NG15 with IGW, one needs to have a relatively large blue-tilt spectrum between the CMB and PTA scales, so that the tiny tensor perturbations at CMB scales can give a detectable signal at nHz scales [26, 27]. The blue tilt must turn into the red tilt at a certain point in order to evade the BBN bounds and LVK constraints [28]. Then, in [14] and [19], respectively, we showed that the previous scenario is possible if there is an inflationary scenario in which *(i)* the reheating temperature $T_{\rm rh}$ is very low (~ 1 GeV) with a constant tensor spectral tilt $n_{\rm t}$ (analogous to γ in the CPL model); or *(ii)* the reheating temperature is very high with an RPL-like tensor spectral tilt.

In both cases, we were able to find regions of parameter space that are not excluded by BBN, CMB, LVK, and NG15. In Fig. 2, we show two plots from these two works. In the left panel, we can see the constraints for the

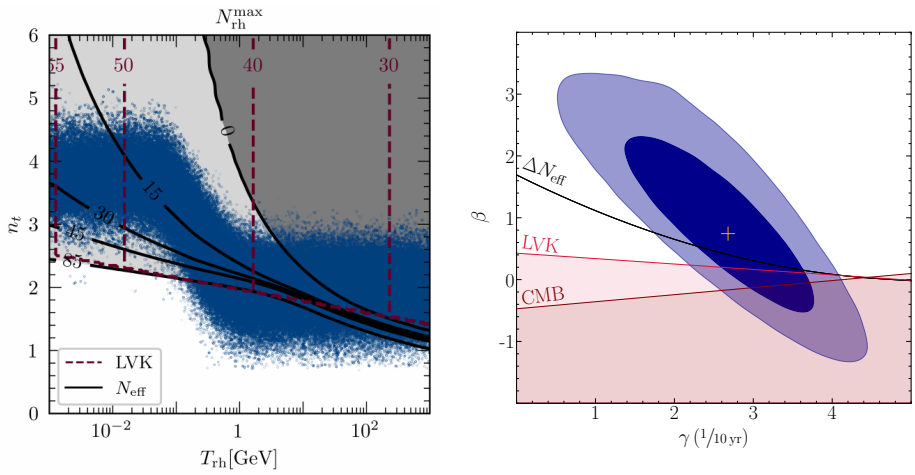

Fig. 2. Left panel: constraints on the parameter space of IGW according to [14]. Right panel: constraints on the RPL parameters if one tries to interpret the RPL model as a phenomenological description of cosmic inflation [19].

IGW model of [14]. The black solid lines show the maximum number of e-folds during reheating that are allowed according to n_t and $T_{\rm rh}$. This has to do with the allowed amount of extra relativistic degrees of freedom $\Delta N_{\rm eff}$. The excluded region is in dark grey. The LVK constraints on the amplitude of the IGW signal are shown as maroon dashed lines. In the right panel, we can see the constraints for the RPL parameters while interpreted as cosmic inflation [19]. This interpretation is only possible if there is a running of the spectral index and is consistent with the 3D MAP point. These bounds are only valid if one assumes that the RPL-like signal (PTA scales) can be extrapolated across a very large range of frequencies (from CMB to LVK).

5. Conclusion

In these proceedings, we briefly reported on the latest searches for the GWB with PTA data, focusing on the New Physics interpretation of NG15. We presented an RPL model-independent description of the signal, as a first step towards the GWB characterisation beyond power-law approaches. Such ideas are common with the CMB data (even up to the running of the running of the spectral index in [29]), but apart from [30], no other work had considered the running of the spectral index in the PTA band. We also highlighted our previous searches for IGW with NG15. Interestingly, we could find scenarios that are not excluded by existing datasets, whether for high or low reheating temperatures. Although not yet conclusive, we can see how the GW data is a powerful tool for constraining many cosmological and New Physics models. The community looks forward to the next datasets.

R.R.L.d.S. is supported in part by the National Science Centre, Poland (NCN) under the research grant No. 2020/38/E/ST2/00126. R.R.L.d.S. acknowledges the reported works were done in collaboration with many other members of the New Physics Working Group of the NANOGrav Collaboration. In particular, the RPL model was developed with the Particle Cosmology Münster group (Kai Schmitz, David Esmyol, Tobias Schröder, and Richard von Eckardstein). R.R.L.d.S. thanks Anish Ghoshal and the organisers of the workshop for the kind invitation.

REFERENCES

[1] LIGO Scientific and Virgo collaborations (B.P. Abbott *et al.*), *Phys. Rev. Lett.* **116**, 061102 (2016).

[2] LIGO Scientific and Virgo collaborations (B.P. Abbott *et al.*), *Phys. Rev. Lett.* **119**, 161101 (2017).

[3] S.R. Taylor, arXiv:2105.13270 [astro-ph.HE].

[4] NANOGrav Collaboration (G. Agazie *et al.*), *Astrophys. J. Lett.* **951**, L9 (2023).
[5] R.W. Hellings, G.S. Downs, *Astrophys. J. Lett.* **265**, L39 (1983).
[6] NANOGrav Collaboration (G. Agazie *et al.*), *Astrophys. J. Lett.* **951**, L8 (2023).
[7] EPTA Collaboration (J. Antoniadis *et al.*), *Astron. Astrophys.* **678**, A50 (2023).
[8] D.J. Reardon *et al.*, *Astrophys. J. Lett.* **951**, (2023).
[9] H. Xu *et al.*, *Res. Astron. Astrophys.* **23**, 075024 (2023).
[10] S. Burke-Spolaor *et al.*, *Astron. Astrophys. Rev.* **27**, 5 (2019).
[11] Event Horizon Telescope Collaboration (K. Akiyama *et al.*), *Astrophys. J. Lett.* **875**, L1 (2019).
[12] NANOGrav Collaboration (G. Agazie *et al.*), *Astrophys. J. Lett.* **952**, L37 (2023).
[13] C. Caprini, D.G. Figueroa, *Class. Quantum Grav.* **35**, 163001 (2018).
[14] NANOGrav Collaboration (A. Afzal *et al.*), *Astrophys. J. Lett.* **951**, L11 (2023).
[15] EPTA and InPTA collaborations (J. Antoniadis *et al.*), *Astron. Astrophys.* **685**, A94 (2024).
[16] D.G. Figueroa, M. Pieroni, A. Ricciardone, P. Simakachorn, *Phys. Rev. Lett.* **132**, 171002 (2024).
[17] J. Ellis *et al.*, *Phys. Rev. D* **109**, 023522 (2024).
[18] LISA Cosmology Working Group (P. Auclair *et al.*), *Living Rev. Relativ.* **26**, 5 (2023).
[19] G. Agazie *et al.*, *Astrophys. J. Lett.* **978**, L29 (2025).
[20] R.R. Lino dos Santos, L.M. van Manen, arXiv:2212.05594 [astro-ph.CO].
[21] NANOGrav Collaboration (A.D. Johnson *et al.*), *Phys. Rev. D* **109**, 103012 (2024).
[22] A. Mitridate *et al.*, arXiv:2306.16377 [hep-ph].
[23] A. Mitridate, «PTArcade», Zenodo, published April, 2023.
[24] J.A. Ellis, M. Vallisneri, S.R. Taylor, P.T. Baker, «ENTERPRISE», Zenodo, published September, 2020.
[25] S.R. Taylor *et al.*, «ENTERPRISE-extensions v2.3.3», https://github.com/nanograv/enterprise_extensions, 2021.
[26] Planck Collaboration (N. Aghanim *et al.*), *Astron. Astrophys.* **641**, A6 (2020); *Erratum ibid.* **652**, C4 (2021).
[27] M. Benetti, L.L. Graef, S. Vagnozzi, *Phys. Rev. D* **105**, 043520 (2022).
[28] LIGO Scientific, Virgo, and KAGRA collaborations (R. Abbott *et al.*), *Phys. Rev. D* **104**, 022004 (2021).
[29] Planck Collaboration (Y. Akrami *et al.*), *Astron. Astrophys.* **641**, A10 (2020).
[30] I. Ben-Dayan, U. Kumar, U. Thattarampilly, A. Verma, *Phys. Rev. D* **108**, 103507 (2023).